Supporting Information

Guy et al. 10.1073/pnas.1110221108

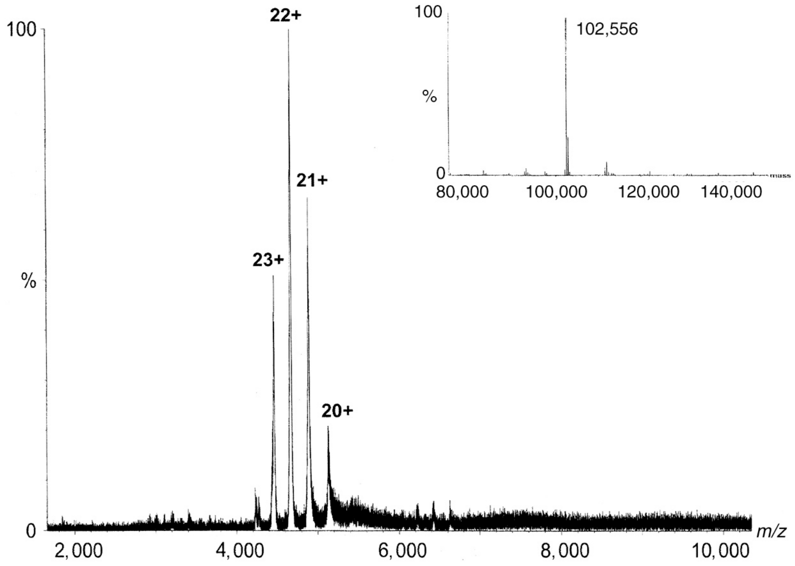

Fig. S1. Electrospray ionization mass spectrum of the sample used for crystallization. The calculated mass of the protein is displayed in the inset. Experimental conditions were as follows: source temperature 120 °C, desolvation gas 120 °C at a flow of 300 L/h, cone voltage 80 V with the electrospray capillary voltage held constant at 3,000 V. The collision cell was pressurized by argon (approximately 15 psi valve setting) and the pumping of the electrospray source region throttled to give an "analyzer" gauge reading of 5.5×10^{-5} mbar and a TOF gauge reading of 4.2×10^{-7} mbar. Horse heart myoglobin (Sigma) was used as an external calibrant. Data were analyzed with the MassLynx 3.5 software package including the Maxent deconvolution algorithm.

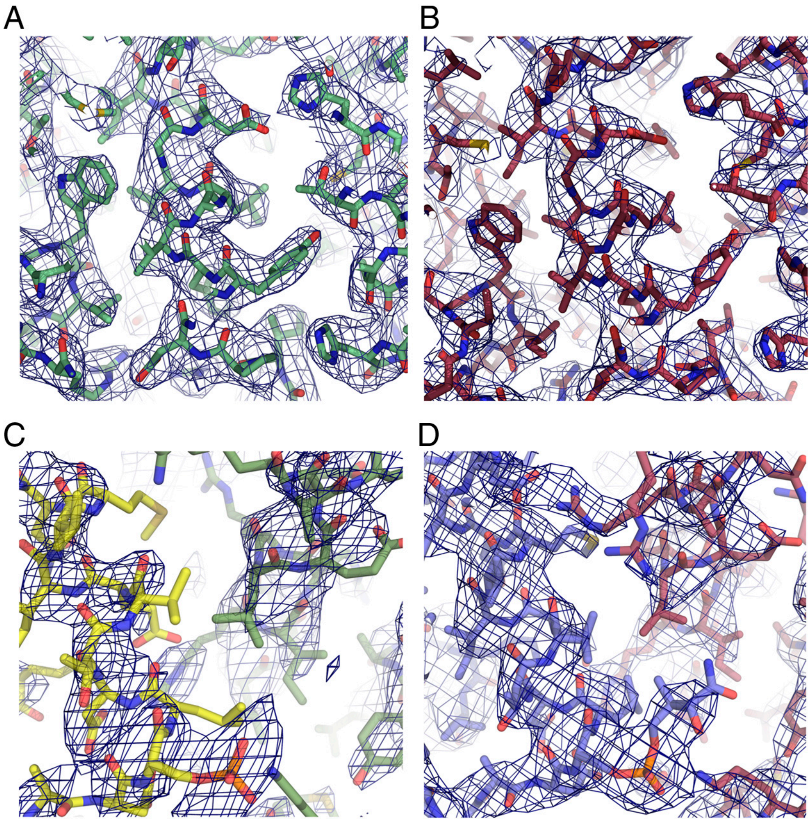

Fig. S2. Electron density ($2F_o - F_c$) maps contoured at 1σ, showing the desaturase itself in (*A*) crystal form 1 and (*B*) crystal form 2, and the desaturase–acyl carrier protein interface in (*C*) crystal form 1 and (*D*) crystal form 2.

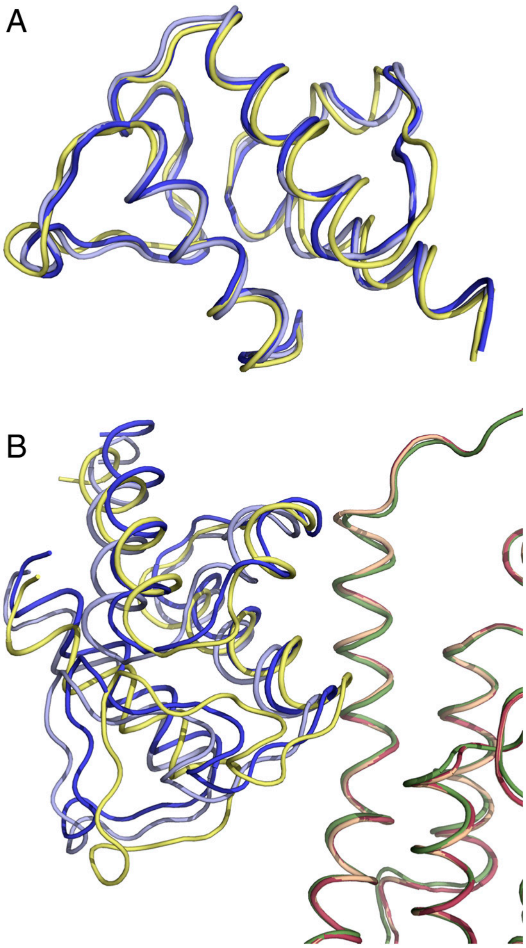

Fig. S3. Similarities and differences in the two crystal forms. *A* shows the superimposed acyl carrier protein (ACP) molecules, chain D from crystal form 1 (yellow), and chains C (dark blue) and D (light blue) from crystal form 2. *B* shows the slightly different orientations of the ACP in each structure, superimposed only by the desaturase, colors are as in *A*.

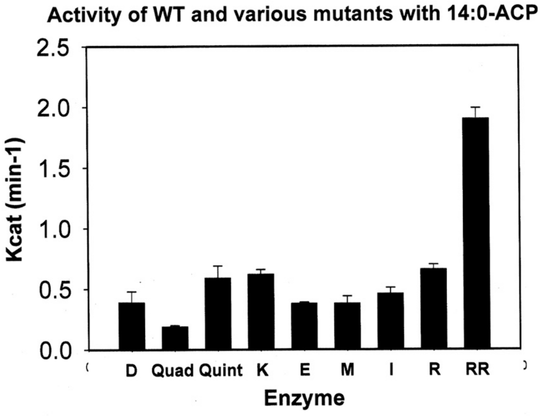

Fig. S4. Activities of WT castor desaturase and mutants thereof described in this work with 14:0-acyl carrier protein (ACP).

Table S1. Regiochemistry of desaturation products of the castor and ivy desaturases with 14:0, 16:0, and 18:0 substrates

	14:1		16:1		18:1	
	Δ4	Δ9	Δ4	Δ9	Δ4	Δ9
Castor	17 (0.6)*	83 (0.6)	ND	100	ND	100
Ivy	100	ND	100	ND	3 (0.5)	97 (0.5)

*Numbers represent percent of product with SD in parenthesis; ND, not detectable with a detection limit of <0.5%.

Table S2. Protein–protein interaction modeling with Haddock

Protein 1	Protein 2	Input surface residues 1	Input surface residues 2	Resulting models	Cluster size	Score	Buried surface area	Complex conformation
Castor desaturase	ACP	260, 262, 280, 333, 340, 344	38	cluster1_3	53	−86	1,161	Δ9
				cluster2_3	141	−79	1,365	unproductive
				cluster3_3	4	−41	1,134	almost Δ9
Ivy desaturase	ACP	255, 257, 275, 328, 335, 339	38	cluster1_5	135	−97	1,465	Δ4
				cluster2_5	15	−62	1,255	unproductive
				cluster3_5	23	−53	1,040	unproductive
				cluster4_5	6	−46	1,141	almost Δ9
				cluster5_5	12	−33	899	tilted Δ9

ACP, acyl carrier protein.

Table S3. Castor desaturase basic residues in the acyl carrier protein (ACP)–desaturase interface and corresponding residues in ivy desaturase

Desaturase species	Specificity		Residues in the observed ACP–desaturase interface							
Castor desaturase	18:0 Δ9	R260	K262	(D280)	R333	R336	L337	R340	R344	K346
Ivy desaturase	16:0 Δ4	R255	K257	(K275)	K328	R331	V332	K335	K339	K341

Residues in parenthesis are only part of the modeled Δ4-complex.

Table S4. Crystallographic data collection and refinement statistics for the two forms of acyl carrier protein (ACP)–desaturase complex crystals

	Crystal form 1	Crystal form 2
Space group	$P3_121$	$P4_322$
Unit cell, Å	188.3, 188.3, 81.3	76.4, 76.4, 403.4
Molecules in asymmetric unit (desaturase)	3	2
Molecules in asymmetric unit (ACP)	1	2
Resolution, Å	30-3.0 (3.16-3.0)	20-3.35 (3.44-3.35)
R_{sym}	0.08 (0.48)	0.073 (0.6)
$\langle I\rangle/\langle\sigma I\rangle$	21.9 (4.3)	9.7 (2.0)
Completeness, %	99.9 (100.0)	94.6 (96.0)
Multiplicity	11.1 (9.6)	2.6 (2.7)
B factor from Wilson plot	87.9	117
Refinement statistics		
Reflections in working set	32,013	16,101
Reflections in test set	1,363	857
$R_{\mathrm{factor}}/R_{\mathrm{free}}$	24.2/27.7	21.2/25.4
No. of protein atoms	9,045	6,910
No. of metal ions	9	6
No. of water molecules	26	0
Avg B factor	98.1	107.3
rmsd from ideals		
Bond lengths, Å	0.013	0.009
Bond angles, °	1.30	1.10
Ramachandran plot		
Preferred regions	96.3%	95.7%
Outliers	0.27%	0.35%

Data in parentheses are for the highest resolution shell.